Int J Ind Chem (2014) 5:111–120
DOI 10.1007/s40090-014-0022-8

RESEARCH

Poly(vinyl alcohol–proline) as corrosion inhibitor for mild steel in 1M hydrochloric acid

A. Ali Fathima Sabirneeza · S. Subhashini

Received: 22 April 2014 / Accepted: 16 September 2014 / Published online: 15 November 2014

Abstract Corrosion inhibitive behavior of newly synthesized water soluble semiconducting polymer composite poly(vinyl alcohol–proline) (PVAP) is focused in this article. The polymer was characterized by FTIR, SEM-EDX, and XRD techniques. Thermogravimetry and differential thermal analysis proved the thermal stability of PVAP. Gravimetry and electrochemical techniques were employed to study the corrosion inhibition performance of PVAP on mild steel in molar hydrochloric acid. 0.6 % (wt.) of PVAP provides a maximum inhibition efficiency of 94 % at 303 K. The role of concentration of PVAP, exposure time and solution temperature on the mild steel corrosion has been investigated. The polarization results showed that PVAP acts as mixed-type inhibitor and could serve as an effective corrosion inhibitor for mild steel in acid medium. Surface morphology of the mild steel specimen by FTIR spectroscopy proved the formation of polymer film.

Keywords Mild steel · Poly(vinyl alcohol–proline) · Weight loss · Polarization · Impedance spectroscopy · Adsorption

Introduction

Steels are the most important engineering materials and cover a wide range of alloys based on iron and carbon. Mild steel (MS) having >2 % carbon is of particular interest due to its high weldability, durability, and easy annealing capacity. MS find its role in almost every product created from metal due to its low cost and easy availability. Hydrochloric acid is the most commonly used pickling acid in industries [1]. The major industries use corrosion inhibitors are oil and gas exploration and production, petroleum refining, chemical manufacturing, water treatment, and the product additive industries to control the metal dissolution and acid consumption.

Industrial corrosion inhibitors are generally of organic or inorganic compounds. Organic inhibitors establish their inhibition via adsorption whereas inorganic compounds act as anodic inhibitors and the metallic atoms enclosed in the film improves its corrosion resistance. The extent of inhibition depends on factors such as functional groups, electronic structure, steric factors [2–4]. The polymer materials are having multiple adsorption sites for bonding with metal surface and provides higher inhibition efficiency than the corresponding monomers [5, 6].

The polymers with higher molecular weight shows higher inhibition efficiency provided the polymers have good solubility [7]. Amino acids are good sources for hetero atoms with non-toxic nature, many literatures revealed the good corrosion inhibition properties of amino acids and its derivatives [8–10] for different metals. Owing to the high cost and biological importance of amino acids, they are not widely used as industrial corrosion inhibitors. Polyvinyl alcohol was reported as a corrosion inhibitor with 50–70 % [11–14] inhibition efficiency depending on the metal–acid system. In our previous communications polyvinyl alcohol was composited with various amino acids like leucine, histidine, threonine, and cysteine which are reported to have more than 92 % inhibition efficiency in 1M HCl [15–17]. The present investigation reports the corrosion inhibition performances of poly(vinyl alcohol–proline) composite.

A. A. F. Sabirneeza (✉) · S. Subhashini
Avinashilingam Institute for Home Science and Higher Education for Women, Coimbatore 641043, Tamil Nadu, India
e-mail: fathima.rahiman@gmail.com

S. Subhashini
e-mail: subhash.sethu@gmail.com

Potentiodynamic polarization, electrochemical impedance spectroscopy, and gravimetric methods were used to explore the enhanced corrosion inhibition of PVAP.

Experimental

Synthesis of poly(vinyl alcohol–proline)

Polyvinyl alcohol (140,000 $gmol^{-1}$) and L-proline (115.13 $gmol^{-1}$) obtained from Merck were used for the synthesis of poly(vinyl alcohol–proline). 10 % solution of PVA in 0.5 M oxalic acid was mixed together with 1 % solution of L-proline in 0.5 M oxalic acid, and the mixture was cooled to 0–5 °C. Freshly prepared ammonium persulfate was added dropwise to the cold mixture with constant stirring. The reaction mixture was stirred well for 2 h using a magnetic stirrer and refrigerated for a day. The solution was made slightly alkaline (pH 8–9) with ammonia solution and the formed polymer composite was precipitated by addition of acetone. PVAP was characterized by FTIR, XRD, and SEM-EDX analysis.

Corrosion measurements

The electrochemical experiments were carried out using frequency response analyzer (Solartron model 1280B) with conventional three electrode system consisting of saturated calomel electrode (SCE) as reference electrode. Platinum foil was used as a counter electrode while mild steel specimens with 1 cm^2 area, and having a composition of (% by weight—0.196 Mn, 0.106 C, 0.027 P, 0.022 Cr, 0.016 S, 0.012 Ni, 0.006 Si, 0.003 Mo, and remainder Fe) was used as a working electrode. Prior to each experiment, the electrodes were immersed in the stagnant solution to attain a steady-state potential.

The gravimetric measurements were performed with the rectangular MS strips (1 × 5 × 0.15 cm) following the ASTM standard procedure [18]. The monitoring parameter is the mass loss resulted from the treatment of MS specimens with the aggressive solution. The corrosion rate surface coverage and inhibition efficiency of PVAP were calculated from the monitoring parameter using the standard relations as explained in our previous communications [15, 16].

The synthesized inhibitor PVAP was characterized using FTIR spectroscopy and XRD techniques. FTIR spectra were done with Bruker-Tensor 27 spectrometer using Attenuated total reflectance (ATR) sampling technique whereas the XRD data were collected with Bruker-AXS GmbH, Karlsruhe, Germany, equipped with a Cu–Kα source, over an angle range of 5°–60° in 2θ with a step width of 0.0167°. The surface morphology of PVAP was recorded using FEI quanta 200 analyzer.

Results and discussions

Characterization of polymer composite

FTIR spectroscopy

The FTIR spectra of PVA, L-proline and that of PVAP are presented in Fig. 1. The FTIR spectrum of pure PVA showed the characteristic absorption bands for O–H, C–H, and C–O peaks. The band observed between 3,500 and 3,200 cm^{-1} are ascribed to the O–H stretching vibration. This band appeared as a broad one due to intermolecular and intramolecular hydrogen bonding in PVA chains. PVA showed vibration band at 3,000–2,800 cm^{-1} which are associated with C–H stretching vibration of the alkyl group. In addition to these bands PVA showed peaks due to C–H bending and deformations in the finger print region (900–500 cm^{-1}). FTIR spectra of proline showed characteristic peaks for N–H and C=O stretching vibrations around 3,400 and 1,720 cm^{-1}, respectively.

PVAP showed the main characteristic band of polyvinyl alcohol at 3,400 cm^{-1} which is due to OH stretching. This absorption band was broadened due to overlapping of NH stretching and the hydrogen bonding between the amide group of the polyamides and the OH group of polyvinyl alcohol. C–N stretching band was observed at 2,148 cm^{-1}. The band at 1,621 cm^{-1} clearly indicates the presence of

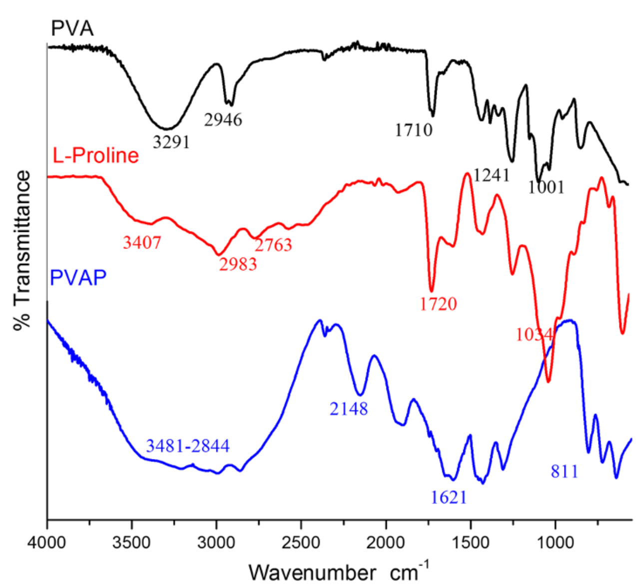

Fig. 1 FTIR spectra of PVA, proline, and PVAP

amide carbonyl group. The absence of the bands in the region 1,730–1,700 cm^{-1} confirms the absence of free carboxylic acid group.

X-ray diffraction studies

The XRD pattern for PVA and PVAP are provided in Fig. 2. The broad band of PVA around 2θ values 20° and 40° due to its semi-crystalline nature. The XRD of PVAP showed several sharp peaks at various 2θ values such as 14, 17.5, 20.5, 22.5, 24, 27.6, 28.6, 29.3, 31.4, 33.8, 34.9, 36.8, 38, 42.4, 45.4, 48.8, 50, and 53. The sharpness of the peak indicates the crystalline nature of PVAP. Moreover, the XRD pattern of PVAP is entirely different from that of PVA which confirms the compositing process.

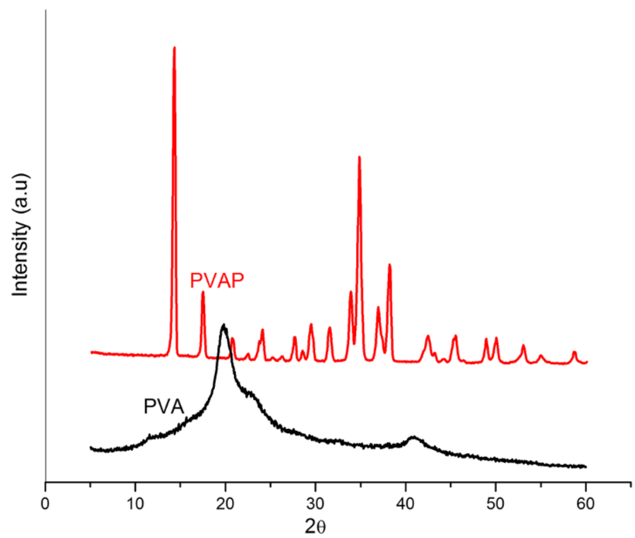

Fig. 2 Scanning electron micrograph of PVAP

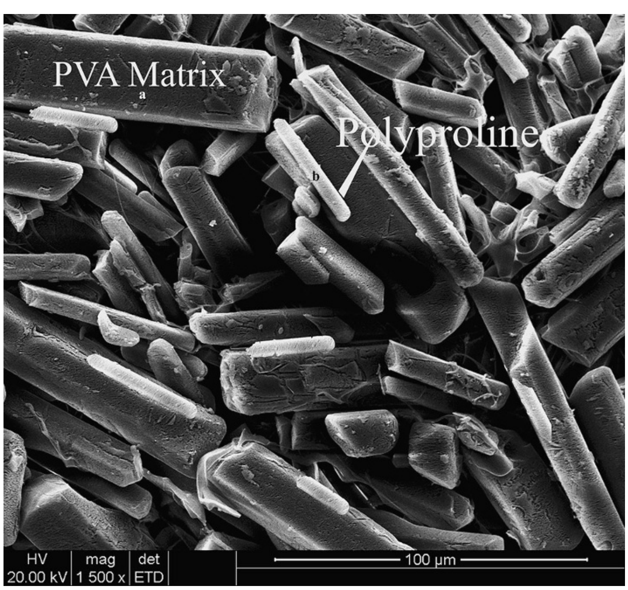

Fig. 3 XRD pattern for PVA and PVAP

Scanning electron microscopy-EDX analysis

The surface morphology of the synthesized polymer composite (Fig. 3) depicts the presence of the binary phase in PVAP. The aminoacid (proline) polymerized and randomly distributed on the polyvinyl alcohol matrix. The elemental composition of the focused area and the marked portions (a and b) was taken by EDX analysis and are presented in Table 1. The total nitrogen count of the focused area was around 10.58 wt% nitrogen. The nitrogen count of 'a and b' portions was around 0.02 and 9.82 wt%. This confirmed the compositing of polyproline phase randomly on the PVA matrix.

AC conductance measurement

The polymer composite was first made into a pellet of diameter 11.07 mm having a thickness 2.95 mm. The electrical connection was made using silver paste and copper wires. LCZ analyzer was used to measure the AC conductance of PVAP at the frequency ranging from 3 to 30000 kHz. The conductance of PVAP at different operating frequencies (Fig. 4) is found to be in the range of 10^{-6} to 10^{-4} Scm^{-1}, which lies in the range of

Table 1 Elemental composition from EDX analysis

Elemental count	Total count	Portion 'a'	Portion 'b'
C	69.68	68.11	69.41
N	11.56	00.38	10.28
O	18.76	31.51	20.31

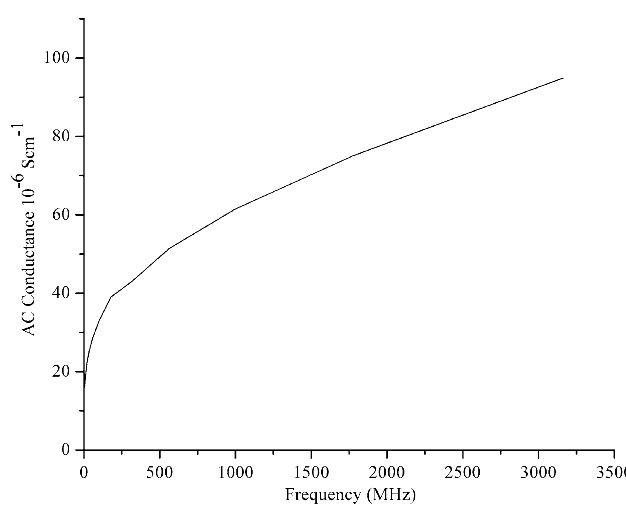

Fig. 4 Variation of AC conductance of PVAP with frequency

semiconductors (10^3 to 10^{-8} Scm^{-1}). The polymer, PVAP differs from the well known conducting polymers such as poly aniline and poly pyrrole. The poly aniline and poly pyrrole are conducting because of the extended aromatic chains through which electron transfer occurs whereas in the case of PVAP such structures are not available. The conductance of PVAP may be due to the presence of large number of amino group which can be easily protonated.

Electrochemical measurements

Potentiodynamic polarization studies

Potentiodynamic polarization measurements were carried out to gain information regarding the kinetics of the anodic and cathodic reactions occur during the corrosion inhibition process. The polarization curves for mild steel in 1M HCl in the absence and presence of various concentrations of PVAP in the potential range of −250 to +250 mV (vs. SCE) at a scan rate of 2 mV/s are shown in Fig. 5. The electrochemical parameters viz. corrosion potential (E_{corr}), corrosion current density (I_{corr}) and Tafel slopes (b_c and b_a) for the corrosion of mild steel in 1M HCl containing different concentrations of PVAP are summarized in Table 2

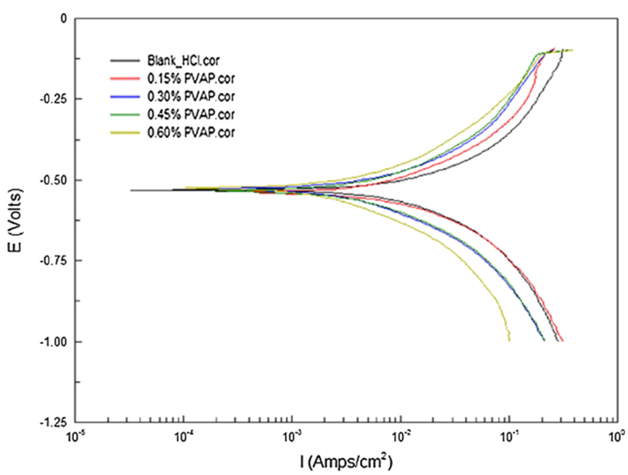

Fig. 5 Potentiodynamic polarization plots for mild steel corrosion in presence of PVAP

along with the calculated inhibition efficiencies (IE_{Icorr}) of PVAP. As the concentration of PVAP increases the cathodic and anodic curves are shifted and corresponding changes in the Tafel slope values indicated that the inhibitor controlled both the cathodic and anodic reactions without affecting reaction mechanism [19].

On the addition of PVAP, the E_{corr} values did not change significantly. Moreover, the displacements in E_{corr} values are found to be less than 85 mV and hence PVAP is regarded as mixed-type inhibitor according to Riggs 1973 classification [20]. Even a very low concentration of PVAP reduces the current density to a considerable value. The suppression in current density increases (12.87–2.75 mA/cm^2) as the concentration of the PVAP increases indicating more and more surface is covered by the inhibitor molecules.

Linear polarization resistance was calculated using the Stern–Geary theory for the potential range of −0.02 to +0.02 mV with respect to the open circuit potential and is presented in Table 2. It is clearly observed that in presence of PVAP the linear polarization resistance increases considerably which increases the inhibition efficiency, IE_{Rp} (Table 2).

AC impedance studies

Impedance measurements of the mild steel electrode at its open circuit potential in 1M HCl with and without PVAP were performed over the frequency range of 20 kHz to 0.1 Hz. The Nyquist and Bode representations of the impedance response of mild steel electrode in the absence and presence of PVAP are shown in Figs. 6 and 7, respectively. It is clear from the Nyqist representations that the plots are not perfect semicircles and this may be due to the frequency dispersion [21]. The experimental data are fitted with the equivalent circuit containing constant phase element, CPE shown in Fig. 6. A phase angle shift at higher frequencies was observed in Fig. 7 with the successive addition of PVAP. This phase angle shift indicates the change in the electrode interfacial structure on the addition of the inhibitor. The continuous increase in the phase angle shift in the presence of the inhibitor was

Table 2 Polarization parameters for mild steel acid corrosion in absence and presence of various concentrations of PVAP

Conc. of PVAP (%)	Tafel extrapolation method (TEM)					LPR method	
	b_a (mV/dec)	b_c (mV/dec)	*E*corr (mV vs. SCE)	I_{corr} (mA/cm^2)	IE_{Icorr} (%)	R_p (Ω cm^2)	IE_{Rp} (%)
Blank	218.26	177.73	−531.88	12.87	–	3.29	–
0.15	172.31	162.18	−537.98	7.92	38.46	4.13	20.33
0.30	188.66	145.20	−529.01	4.72	63.33	6.99	52.93
0.45	169.86	151.38	−531.43	4.52	64.89	7.58	56.60
0.60	191.11	133.86	−524.06	2.75	78.63	11.26	70.78

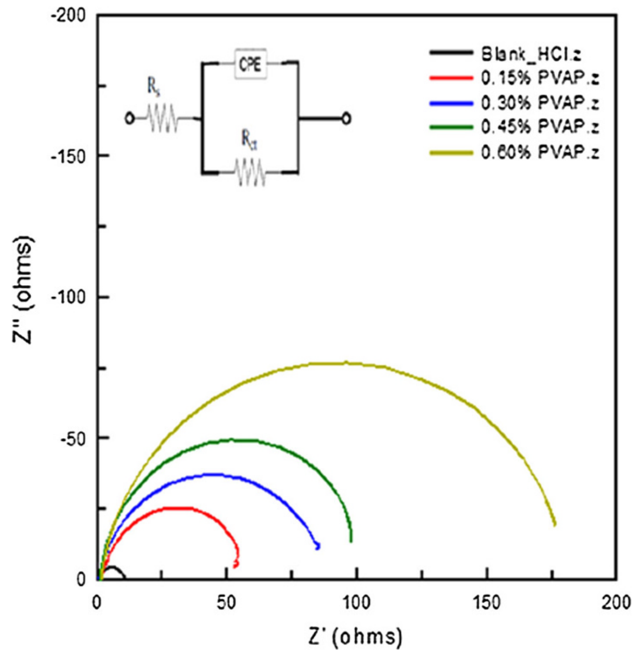

Fig. 6 Nyquist plots for mild steel corrosion in 1M HCl in presence of PVAP

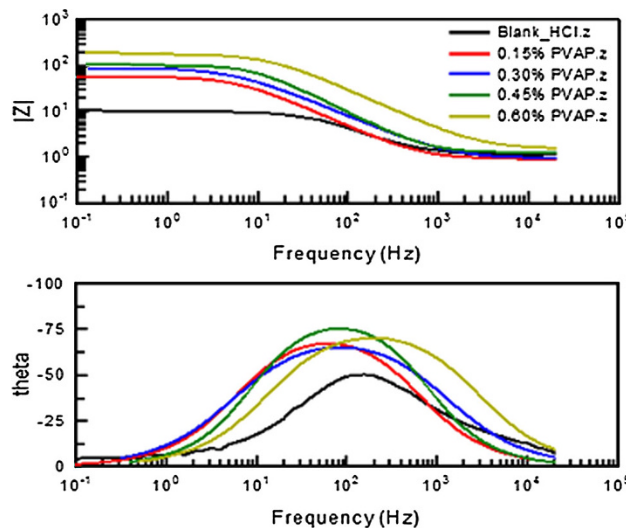

Fig. 7 Bode plots for mild steel corrosion in 1M HCl in presence of PVAP

obviously correlated with the inhibitor film growth and with the increase in inhibitor coverage on the mild steel surface. The simulations are carried out to minimize the chi-squared valued to 10^{-2}. This technique is useful in the determination of the double layer capacitance and charge transfer resistance of the system. The various impedance parameters such as charge transfer resistance, R_{ct} and double layer capacitance, C_{dl} are presented in Table 3. As the concentration of PVAP increases the R_{ct} value increases from 9.37 to 180.96 Ωcm^{-2} whereas the C_{dl} value decreases from 452 to 82 μF. This is attributed to the increase in the surface coverage by the inhibitors leading to an increase in inhibition efficiency to about 95 %. A decrease in the local dielectric constant and/or an increase in the thickness of the electrical double layer are responsible for the decrease in C_{dl} values. The changes in R_{ct} and C_{dl} values were caused by the gradual replacement of water molecules by the polymer on the metal surface which decreases the extent of metal dissolution [22].

Weight loss method

Weight loss, corrosion rate, and inhibition efficiency

During the corrosion process, the mild steel undergoes dissolution leading to base metal loss. Thus, it is conventional to monitor the mass loss of the metal coupons before and after acid treatment to measure the corrosion rate. The performance of PVAP inhibitor against uniform corrosion was thus investigated with immersion tests by monitoring the metal loss. The obtained mass loss was used to calculate corrosion rate, surface coverage and inhibition efficiency. The calculated parameters are provided in Table 4. The variation of inhibition efficiency with immersion time for different concentrations of PVAP is shown in Fig. 8. The figure also includes the inhibition efficiencies obtained for 0.6 weight percent of PVA (for the selected immersion period) which was only 72.5 %. On compositing 0.0047 mol of proline with polyvinyl alcohol increases the inhibition efficiency to 94.2 %. It is also apparent that the inhibition efficiency has increased from 78 to 94 % as the concentration of PVAP was increased from 0.06 to 0.6 % by weight. The maximum inhibition efficiency was observed at 0.6 % PVAP (by weight) and any further increase in concentration did not cause any appreciable change in the performance of the inhibitor thereby indicating the attainment of the limiting value. This effect may be due to the adsorption of the polymer composite onto the metal surface, which reduces the direct contact of the metal from the corrosive environment. The higher performance of PVAP is attributed to the presence of nitrogen and oxygen atoms, larger molecular size and linearity in the polymeric chain. As the immersion time increases, the inhibition performance also increases. The maximum IE value was obtained for 6 h, after that slight decrease in IE_w was observed. As the time passes on the stability of adsorbed film decreases and results in desorption to attain the equilibrium.

Effect of temperature

Hydrochloric acid is the most important pickling acid used with concentrations raging from 5 to 15 mass% up to

Table 3 Electrochemical impedance parameters for mild steel in 1M HCl in absence and presence of various concentrations of PVAP

Conc. of PVAP (%)	Chi-Sqr χ^2	Double layer capacitance C_{dl} (μF)	Surface coverage θ	Charge transfer RESISTANCE R_{ct} (Ω cm^2)	Inhibition efficiency IE_{Rct} (%)
Blank	0.00934	452	–	9.37	–
0.15	0.00981	322	0.2876	54.23	82.72
0.30	0.00542	303	0.3296	88.03	89.35
0.45	0.00214	253	0.4402	100.09	90.64
0.60	0.00742	82	0.8185	180.96	94.82

Table 4 Corrosion rate (mpy) and surface coverage for mild steel corrosion in 1M HCl in the absence and presence of different concentrations of PVAP at different immersion periods

Conc. of PVAP (%)	Corrosion rate (mpy)					Surface coverage				
	1 h	3 h	6 h	12 h	24 h	1 h	3 h	6 h	12 h	24 h
0.00	1822.90	3693.42	3831.86	3944.53	3309.24	–	–	–	–	–
0.12	517.65	714.62	570.27	1170.2	861.31	0.71	0.81	0.85	0.70	0.74
0.24	435.22	542.65	482.39	1008.8	828.13	0.76	0.85	0.87	0.74	0.75
0.36	376.79	427.96	342.77	938.99	795.69	0.79	0.88	0.91	0.76	0.76
0.48	285.64	335.65	280.55	878.55	725.52	0.84	0.90	0.93	0.78	0.78
0.60	255.55	249.27	230.19	812.01	684.75	0.86	0.94	0.94	0.79	0.79

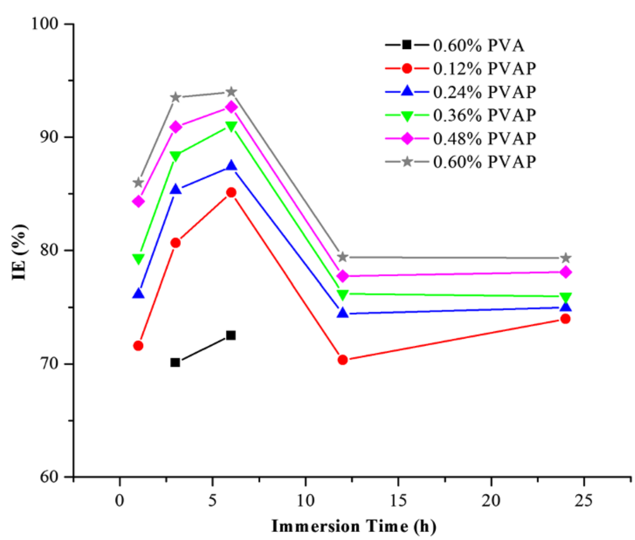

Fig. 8 Variation of inhibition efficiency of PVA and PVAP with immersion time

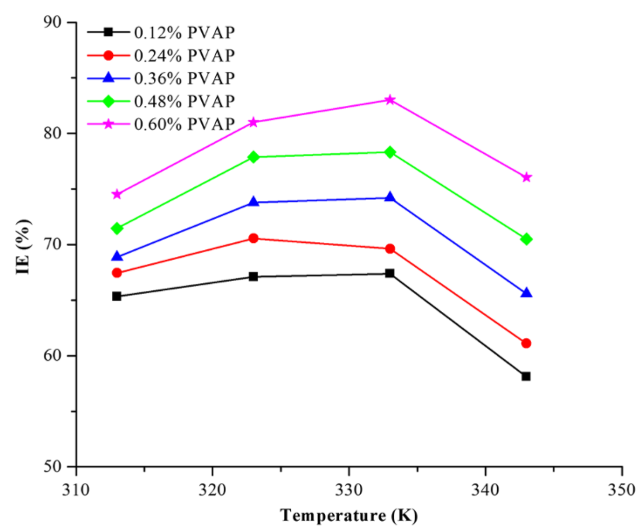

Fig. 9 Variation of inhibition efficiency of PVAP with immersion temperature

80 °C. The higher temperature can influence the corrosive interaction exist between the mild steel and the acidic medium in the absence and presence of the inhibitors. The performance of PVAP toward acid corrosion of mild steel at higher temperatures was studied, and the obtained results are shown in Fig. 9. The inhibition efficiency increases with temperature up to 50 °C, which indicates the stability of the adsorbed film at the studied temperatures. The increase in IE_w up to 50 °C may be due to the increased adsorption involving chemical interactions between PVAP and mild steel. With further increase in temperature, inhibition efficiency decreases which indicate the instability of the adsorbed film above 50 °C. Similar type results were observed for the other amino acid polyvinyl alcohol composites [16, 17]. The increased hydrogen liberation caused the adsorbed polymer film to peel off from the metal surface there by exposing the base metal to acid which is susceptible for the corrosion attack. This results in higher corrosion rate at higher temperature thereby decreasing the inhibition efficiencies above 50 °C.

Corrosion kinetic parameters

Arrhenius suggested the famous relation which relates the temperature dependence on the rate of the reaction [23, 24].

$$\log \mathrm{CR} = \frac{-E_a}{2.303RT} + \log \lambda, \quad (7)$$

where, CR is the corrosion rate, E_a is the apparent activation energy, λ is the Arrhenius pre exponential factor, R is the gas constant ($R = 8.314\ \mathrm{JK^{-1}mol^{-1}}$), and T is the absolute temperature. The equation predicts the linear relationship between the corrosion rate and temperature (Fig. 10). From the slope and intercept of the plots, the activation energy and the λ values were calculated and are given in Table 5. The data showed that the activation energy for the corrosion of mild steel in 1M HCl in the presence of inhibitor (57.74 kJ/mol) is higher than that in free acid (43.76 kJ/mol). This indicated that the used inhibitors considerably increase the activation energy of the corrosion process due to their adsorption onto the metal surface [25, 26].

In the literature, the lower activation energy value for corrosion process in the presence of the inhibitor is attributed to its chemisorption, while the higher value is associated with its physical adsorption [27]. The increased activation energy in presence of the inhibitor suggests that adsorbed polymer create a physical barrier to charge and mass transfer, leading to lower in corrosion rate [28]. The value of λ is also higher for the inhibited solutions than the uninhibited one. The variation of both E_a and λ with concentration reveals that activation energy is the deciding factor rather than λ.

The transition state equation can be used to calculate the enthalpy (ΔH_o) and entropy of activation (ΔS_o) process for the formation of activated complex in the transition [29].

$$\mathrm{CR} = \frac{RT}{Nh} \exp\left(\frac{\Delta So}{R}\right) \exp\left(-\frac{\Delta Ho}{RT}\right), \quad (8)$$

where, h is the Planck's constant and N is the Avogadro's number. A plot of log (CR/T) versus 1/T (Fig. 11) gave straight lines with slope equals to $-\Delta H_o/2.303R$ and intercept equals to $[\log(R/Nh) + (\Delta S_o/2.303\mathrm{R})]$ from which ΔH_o and ΔS_o were calculated and listed in Table 5.

The enthalpy of activation values is found to be positive in the absence and presence of inhibitor reflects the endothermic mild steel dissolution process. It is evident from the

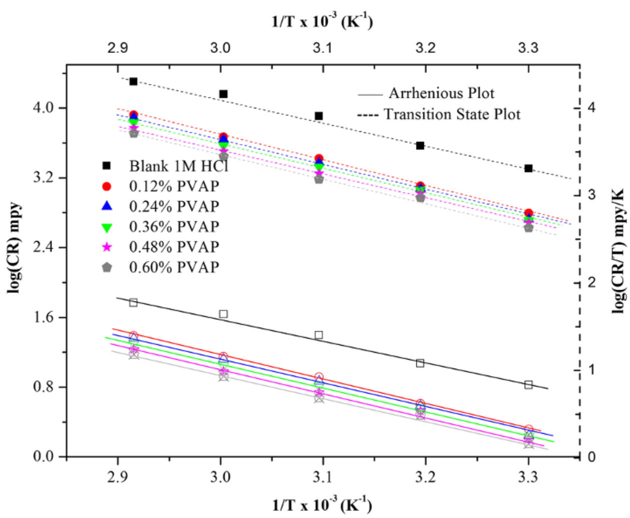

Fig. 10 Arrhenious and transition state plots for mild steel corrosion in 1N HCl containing various concentrations of PVAP

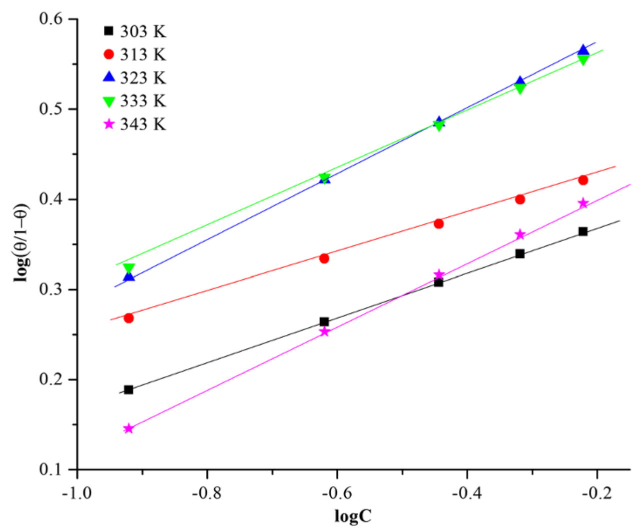

Fig. 11 El-Awady isotherm for PVAP adsorption on mild steel

Table 5 Activation parameters of mild steel corrosion in presence of PVAP in 1M HCl

Conc. of PVAP (%)	E_a (kJ/mol)	λ 10^{12}	ΔH_o (J/mol)	ΔS_o (J/Kmol)	$+\Delta G_o$ (kJ/mol)				
					30 °C	40 °C	50 °C	60 °C	70 °C
Blank	43.76	1.58	48.87	−40.86	11.37	11.72	12.09	12.46	12.84
0.12	52.80	3.10	50.11	−37.27	12.53	12.95	13.36	13.77	14.18
0.24	52.48	4.98	53.53	−41.21	12.40	12.81	14.09	13.62	15.97
0.36	55.05	36.00	52.36	−46.60	14.11	14.57	15.04	15.50	18.71
0.48	56.21	42.73	55.05	−54.40	16.53	17.07	17.62	18.16	19.43
0.60	57.74	92.75	54.49	−59.10	17.17	17.73	19.14	19.73	20.32

table that the value of ΔH_o increased in the presence of PVAP than the uninhibited solution indicating higher protection efficiency. This suggested the slow dissolution and hence lower corrosion rate of mild steel [30]. Comparing the values ΔS_o it is clear that the entropy of activation decreased in the presence of the studied inhibitor than that of the free acid. The low value of ΔS_o supports the slower metal dissolution in the presence of PVAP.

The change in free energy of activation (ΔG_o) of the corrosion process can be calculated at each temperature applying the basic thermodynamic relation,

$$\Delta G_o = \Delta H_o - T\Delta S_o. \quad (9)$$

The calculated ΔG_o values at each temperature are listed in Table 5. The values were positive and increased with increase in temperature. With increase in temperature, the spontaneity of the corrosion process increases indicating that the activated complex was not stable at higher temperatures. With the increase in concentration the free energy of activation increases results from the unstable activated complex at the rate determining transition state.

Adsorption isotherm and adsorption parameters

The basic information regarding the interactions between the inhibitor molecules and also with the mild steel surface can be revealed with the help of adsorption isotherms. For PVAP, the experimental surface coverage values at different temperatures were fitted to various isotherm models including Langmuir, Temkin, Frumkin, and Flory–Huggins. By far the tested models the best fit was obtained with the Langmuir isotherm which has been extensively used in the literatures for various metal inhibitor systems in acidic media [31, 32]. According to this isotherm, θ is related to C_{inh} by the relation,

$$K \cdot C_{inh} = \frac{\theta}{1-\theta}, \quad (10)$$

where, K is the equilibrium constant of the adsorption–desorption process. Figure 10 represents the Langmuir isotherm for the studied polymer composite at different temperatures and their corresponding parameters are summarized in Table 6.

From the intercept of the lines the equilibrium constant, K is calculated which is related to the standard free energy of adsorption, ΔG_{ads} by the following equation [29],

$$K = \frac{1}{55.5}\exp\left(\frac{-\Delta G_{ads}}{RT}\right), \quad (11)$$

where, R is gas constant in $JK^{-1}mol^{-1}$ and T is absolute temperature. The value 55.5 is the concentration of water in solution. The values of ΔG_{ads} on mild steel at various temperatures are calculated and presented in Table 6. The

Table 6 Adsorption parameters of mild steel corrosion in presence of PVAP in 1M HCl

Temp (K)	R^2	Slope	K	ΔG_{ads} (kJ/mol)	ΔH_{ads} (kJ/mol)	ΔS_{ads} (J/Kmol)
303	0.9994	0.8440	20.73	−17.76		
313	0.9986	0.8678	24.87	−18.82	−10.84[a]	24.15[a]
323	0.9984	0.9546	18.91	−18.68	−16.66[b]	18.22[b]
333	0.9985	0.9513	19.10	−19.29		
343	0.9965	0.8999	12.45	−18.65		

[a] Parameters calculated from Van't Hoff equation

[b] Parameters calculated from basic thermodynamic equation

ΔG_{ads} values for PVAP adsorption on mild steel were found to be negative suggesting its spontaneous adsorption [33]. The values of ΔG_{ads} are less than −20 kJ/mol reflecting the physisorption of PVAP.

Van't Hoff equation was used to calculate the other important thermodynamic parameters such as enthalpy (ΔH_{ads}) and entropy of adsorption (ΔS_{ads}) as per the relation [34].

$$\ln K = -\frac{\Delta H_{ads}}{RT} + \frac{\Delta S_{ads}}{R} + \ln\frac{1}{55.5} \quad (12)$$

The plot of ln K against $1/T$ (Fig. 12) yields straight line with slope equals to ($-\Delta H_{ads}/R$) and intercept equals to ($\Delta S_{ads}/R$ + ln 1/55.5). The resulted enthalpy and entropy of adsorption are presented in Table 6. The enthalpy of adsorption was found to be negative (−10.84 kJ/mol) indicating the exothermic adsorption of PVAP. The ΔS_{ads} value is positive which attributed to the exothermic adsorption process accompanied by the increase in entropy [35].

The enthalpy and entropy of adsorption were also calculated from the plot of ΔG_{ads} against T according to the basic

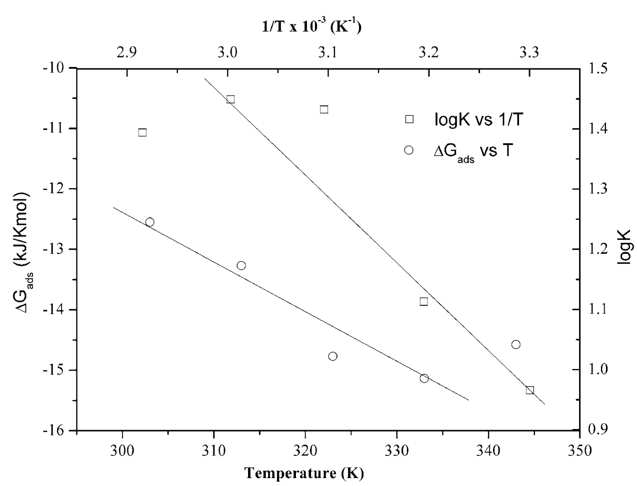

Fig. 12 Plots of lnK against $1/T$ and ΔG_{ads} vs. T for PVAP adsorption on mild steel

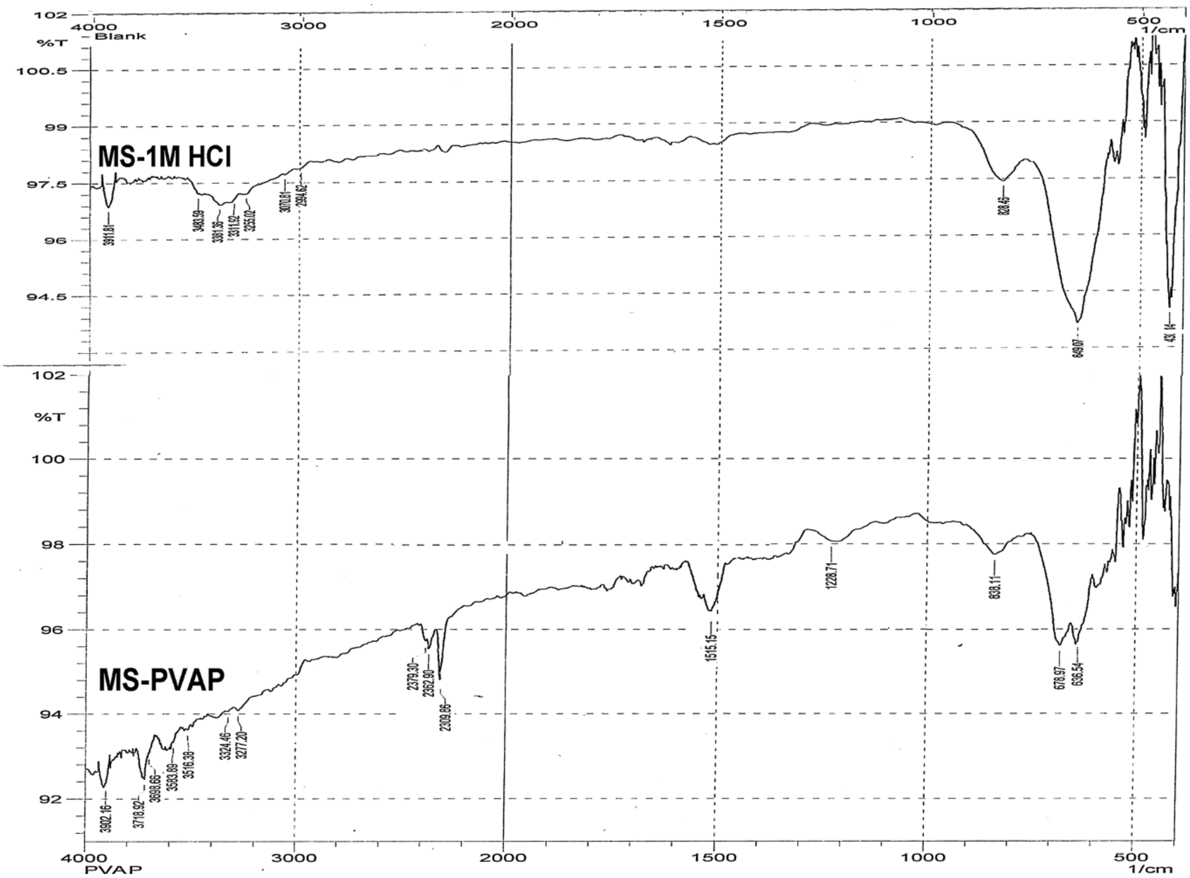

Fig. 13 FTIR spectra of mild steel treated with 1M HCl and 1M HCl containing PVAP

thermodynamic relation (Fig. 13). From the slope and intercept of the straight line, entropy and enthalpy of adsorption values are calculated (Table 6) which are in good agreement with the Van't Hoff's enthalpy and entropy of adsorption. These results corroborated a strong adsorption of the polymer composite on the metal surface [35].

Surface analysis

The surface analyses of the mild steel specimens after treatment with 1M HCl in the absence and presence of PVAP were carried out to confirm the adsorption of the polymer composite on the mild steel specimens. Figure 13 represents the FTIR spectra of corroded mild steel and the PVAP treated mild steel. The corroded surface shows peaks at 3,480–3,255 and 649 cm^{-1} corresponding to that of Fe_2O_3. In case of polymer-treated mild steel, appearance of peaks around 3,710, 3,583, 2,360, and 1,515 cm^{-1} confirms the adsorption of PVAP on the metal surface. Moreover the intensity of the peaks corresponds to Fe_2O_3 has been reduced indicating less pronounced attack of the acid on MS in presence of PVAP. This confirmed the absorption of polymer composite onto the metal surface.

Conclusions

The studied PVAP shows excellent inhibition properties toward mild steel acid corrosion. The inhibition efficiencies obtained in potentiodynamic polarization, impedance, and gravimetric methods are in good agreement with each other. The polarization studies proved PVAP to be a mixed-type inhibitor. The corrosion parameters changed drastically on the addition of PVAP in such a way to increase the inhibition efficiency with concentration and immersion time. The activation parameters reflect the endothermic metal dissolution process. The adsorption of PVAP follows the Langmuir isotherm model and the values of the free energy of adsorption indicate its spontaneous physical nature. FTIR studies confirmed the adsorption of PVAP on the mils steel surface.

Acknowledgments The authors wish to thank Avinashilingam Institute for Home Science and Higher Education for Women, Coimbatore for providing the lab facility. One of the authors Ali Fathima is thankful to CSIR—New Delhi, for Research Fellowship.

References

1. Ahamad I, Quraishi MA (2010) Mebendazole: new and efficient corrosion inhibitor for mild steel in acid medium. Corros Sci 52:651–656
2. Jayalakshmi M, Muralidharan VS (1998) Correlation between structure and inhibition of organic-compounds for acid corrosion of transition-metals. Ind J Chem Tech 5:16–28
3. Granese SL (1998) Study of the inhibitory action of nitrogen-containing compounds. Corrosion 44:322–329
4. Granese SL, Rosales BM, Oviedo C, Zebrino JO (1992) The inhibition action of heterocyclic nitrogen organic compounds on Fe and steel in HCl media. Corros Sci 33:1439–1453
5. Jeyaprabha C, Sathiyanarayanan S, Phani KLN, Venkatachari G (2005) Influence of poly(aminoquinone) on corrosion inhibition of iron in acid media. Appl Surf Sci 252:966–975
6. Jeyaprabha C, Sathiyanarayanan S, Phani KLN, Venkatachari G (2005) Investigation of the inhibitive effect of poly(diphenylamine) on corrosion of iron in 0.5 M H2SO4 solutions. J Electroanal Chem 585:250–255
7. Small PA (1953) Some factors affecting the solubility of polymers. J Appl Chem 3:71–80
8. Yurt A, Bereket G, Ogretir C (2005) Quantum chemical studies on inhibition effect of amino acids and hydroxy carboxylic acids on pitting corrosion of aluminium alloy 7075 in NaCl solution. J Mol Struc THEOCHEM 725:215–221
9. Taha AA, Selim IZ, Khedr AA (1995) Evaluation of some amino acids as corrosion inhibitor for steel in sulphuric solutions at different temperatures. Egypt J Chem 38:141–149
10. Ashassi-Sorkhabi H, Majidi MR, Seyyedi K (2004) Investigation of inhibition effect of some amino acids against steel corrosion in HCl solution. Appl Surf Sci 225:176–185
11. Khairou KS, El-Sayed A (2003) Inhibition effect of some polymers on the corrosion of cadmium in a hydrochloric acid solution. J Appl Polym Sci 88(4):866–871
12. Umoren SA, Ebenso EE, Okafor PC, Ogbobe O (2006) Water-soluble polymers as corrosion inhibitors. Pigm Resin Technol 35:346–352
13. Ebenso EE, Ekpe UJ, Umoren SA, Jackson E, Abiola OK, Oforka NC (2006) Synergistic effect of halide ions on the corrosion inhibition of aluminum in acidic medium by some polymers. J Appl Polym Sci 100(4):2889–2894
14. Umoren SA, Ogbobe O, Okafor PC, Ebenso EE (2007) Polyethylene glycol and polyvinyl alcohol as corrosion inhibitors for aluminium in acidic medium. J Appl Polym Sci 105(6):3363–3370
15. Ali Fathima Sabirneeza A, Subhashini S, Rajalakshmi R (2013) Water soluble conducting polymer composite of polyvinyl alcohol and leucine: An effective acid corrosion inhibitor for mild steel. Mater Corros 64:74–82
16. Ali Fathima Sabirneeza A, Subhashini S (2013) A novel water-soluble, conducting polymer composite for mild steel acid corrosion inhibition. J Appl Poly Sci 127:3084–3092
17. Subhashini S, Sabirneeza AA (2011) Gravimetric and electrochemical investigation of water soluble poly(vinyl alcohol-threonine) as corrosion inhibitor for mild steel. In: Proceedings of WCECS, San Francisco, USA, vol-II, pp 657–662
18. ASTM G 1-2 (1996) Wear and erosion; metal corrosion, Annual book of ASTM standards, vol 0.3.02. ASTM, West Conshohocken, pp 89–95
19. Hassan HH, Abdelghani E, Amin MA (2007) Inhibition of mild steel corrosion in hydrochloric acid solution by triazole derivatives: part I. Polarization and EIS studies. Electrochim Acta 52:6359–6366
20. Riggs OL Jr (1973) Corrosion Inhibitors, 2nd edn. C. C. Nathan, Houston
21. Abdel-Rehim SS, Khaled KF, Abd-Elshafi NS (2006) Electrochemical frequency modulation as a new technique for monitoring corrosion inhibition of iron in acid media by new thiourea derivative. Electrochim Acta 51:3269–3277
22. Quraishi MA, Sardar R (2003) Hector bases—a new class of heterocyclic corrosion inhibitors for mild steel in acid solutions. J Appl Electrochem 33:1163–1168
23. Breslin CB, Carrol WM (2003) The activation of aluminium by indium ions in chloride, bromide and iodide solutions. Corros Sci 34:327–341
24. Khedr MGA, Lashien MS (1992) The role of metal cations in the corrosion and corrosion inhibition of aluminium in aqueous solutions. Corros Sci 33:137–151
25. Negm NA, Salem MAI, Zaki MF (2009) Solubilization behaviors of nonpolar substrates using double tailed cationic surfactants. J Dis Sci Tech 30:1167–1174
26. Negm NA, Zaki MF (2008) Corrosion inhibition efficiency of nonionic Schiff base amphiphiles of *p*-aminobenzoic acid for aluminum in 4N HCl. Colloid Surf A Physiochem Eng Aspec 322:97–102
27. Labrabi L, Harek Y, Benali O, Ghalem S (2005) Hydrazide derivatives as corrosion inhibitors for mild steel in 1M HCl. Prog Org Coat 54:256–262
28. Oguzie EE (2006) Studies on the inhibitive effect of *Occimum viridis* extract on the acid corrosion of mild steel. Mater Chem Phys 99:441–446
29. Bentiss F, Lebrini M, Lagrenee M (2005) Thermodynamic characterization of metal dissolution and inhibitor adsorption processes in mild steel/2,5-bis(*n*-thienyl)-1,3,4-thiadiazoles/hydrochloric acid system. Corros Sci 47:2915–2931
30. Benali O, Larabi L, Tabti B, Harek Y (2005) Influence of 1-methyl 2-mercapto imidazole on corrosion inhibition of carbon steel in 0.5M H_2SO_4. Anti Corros Method Mater 52:280–285
31. Bentiss F, Traisnel M, Chaibi N, Mernari B, Vezin H, Lagrenee M (2002) 2,5-Bis(*n*-methoxyphenyl)-1,3,4-oxadiazoles used as corrosion inhibitors in acidic media: correlation between inhibition efficiency and chemical structure. Corros Sci 44:2271–2289
32. Lagrenee M, Mernari B, Bouanis M, Traisnel M, Bentiss F (2002) Study of the mechanismand inhibiting efficiency of 3,5-bis(4-methylthiophenyl)-4H-1,2,4-triazole on mild steel corrosion in acidic media. Corros Sci 44:573–588
33. Ebenso EE, Obot IB (2010) Inhibitive properties, thermodynamic characterization and quantum chemical studies of secnidazole on mild steel corrosion in acidic medium. Int J Electrochem Sci 5:2012–2035
34. Musa AY, Khadum AAH, Mohamad AB, Daud AR, Takriff MS, Kamarudin SK (2009) A comparative study of the corrosion inhibition of mild steel in sulphuric acid by 4,4-dimethyloxazolidine-2-thione. Corros Sci 51:2393–2399
35. Gomma MK, Wahdan MH (1995) Schiff bases as corrosion inhibitors for aluminiumin hydrochloric acid solution. Mater Chem Phys 39:209–213